In-plane flux pinning in melt-textured $YBa_2Cu_3O_7$-Y_2BaCuO_5 composites

B. Martínez, T. Puig, A. Gou, V. Gomis, S. Piñol, J. Fontcuberta, and X. Obradors
Institut de Ciència de Materials de Barcelona-Consejo Superior de Investigaciones Científicas, Campus Universitat Autònoma de Barcelona, Bellaterra 08193 Spain

G. Chouteau
High Magnetic Field Laboratory, 25 Avenue des Martyrs, Boîte Postale 166, F-38042 Grenoble Cedex 9, France
(Received 20 April 1998; revised manuscript received 28 July 1998)

The critical currents of a series of $YBa_2Cu_3O_7/Y_2BaCuO_5$ (123-211) melt-textured ceramic composites have been measured inductively with the field applied parallel to the *ab* planes ($H\|ab$) and compared to those previously analyzed when $H\|c$. In-plane vortex pinning mechanisms are analyzed from temperature and field dependence of $J_c^c(H\|ab)$ in samples with different concentration of 211 particles. A hierarchy of pinning centers has been identified and analyzed: 123/211 interfaces, dislocations, stacking faults, and twin boundaries. We show that the interface of the secondary phase Y_2BaCuO_5 with the superconducting matrix plays an important role in pinning the Josephson vortices though with a reduced efficiency as compared to Abrikosov vortices. In addition, we identify a second contribution to flux pinning which is independent of V/d, i.e., the amount of interface between the Y_2BaCuO_5 particles and the matrix, that we associate with in-plane linear defects, such as dislocations and partial dislocations surrounding the stacking faults. Finally, the contribution to the pinning of Josephson vortices from twin planes has also been evaluated. [S0163-1829(98)03446-8]

I. INTRODUCTION

Melt-textured $YBa_2Cu_3O_7/Y_2BaCuO_5$ (123-211) superconducting composites have been attracting considerable attention since the discovery that, through directional solidification processes,[1] the main factor limiting the critical currents in ceramic superconductors, i.e., high angle grain boundaries, could be avoided. Under these conditions high critical currents have been achieved surpassing even those obtained in 123 single crystals. Any further enhancement of the critical currents in melt-textured growth (MTG) superconductors relies on the ability to understand which are the flux-pinning mechanisms and how they are related to the microstructure of the ceramic 123/211 composites.[2]

Investigations of the microstructure of 123/211 MTG composites by TEM (Refs. 3 and 4) have evidenced the complexity of these materials where several kinds of defects coexist and interact. Nowadays, a considerable systematic investigation of the formation and evolution of these defects has been settled and it has been particularly rewarding that their geometrical arrangement follows clear patterns. It has been established that the defects which may play a role in the flux-pinning problem can be classified as: (1) second phase precipitates such as 211 particles with a quasispherical geometry, (2) planar defects lying parallel to the *c* axis, twin boundaries for instance, and (3) linear and planar defects lying parallel to the *ab* plane: stacking faults, dislocations, and microcracks. The knowledge of the detailed structure and formation mechanisms of these defects enables us now to analyze one of the most outstanding problems of high-temperature superconductors: their anisotropic behavior.

In a recent work,[5] we analyzed systematically the critical currents of a whole set of samples with different amounts of 211 particles when $H\|c$. There, we demonstrated that the 123/211 interface plays a dominant role in the pinning behavior of the superconducting composites, but it was also concluded that secondary defects should not be neglected in certain regions of the magnetic phase diagram. The collective interaction between vortices was shown to limit the effectiveness of these interfaces in the enhancement of the total pinning force. The understanding of the anisotropy of the flux-pinning mechanisms in 123/211 composites is still incomplete and a systematic analysis of the relationship among the nature of the vortex state in $YBa_2Cu_3O_7$ (YBCO) and the complex microstructure of 123/211 textured ceramics is required.

In layered superconducting cuprates,[6] a crossover from two-dimensional (2D) to 3D vortex nature occurs when the Ginzburg-Landau coherence length along the *c* axis extends beyond the separation of the CuO_2 planes. This crossover temperature T_{cr} is defined by $\xi_c(T_{cr})=\varepsilon\xi_{ab}(T_{cr})=d/\sqrt{2}$, where d is the separation among CuO_2 planes and ε is the mass anisotropy ratio $\varepsilon=(m_{ab}/m_c)^{1/2}$. At low temperatures ($T<T_{cr}$), and depending on the orientation of H with respect to the CuO_2 planes, the usual rectilinear vortex structure breaks down in a kinked vortex state which consists of pancake vortices with shielding currents lying within the CuO_2 planes and vortex strings (or Josephson vortices) with the phase core having a dimension d along the *c* axis and $\Lambda=d/\varepsilon$ perpendicular to it. This kinked vortex state transforms to a locked state below an angle θ_L and then B is strictly parallel to the CuO_2 planes. In Y123, T_{cr} can be estimated as $\approx$80 K and hence in most of the temperature range usually investigated, the 2D nature of the vortices dominates. In this case depending on the orientation of the Lorentz force F_L, three contributions to bulk pinning must be distinguished in the kinked state: (1) pancake pinning

with $F_L \| ab$, (2) intrinsic pinning with $F_L \| c$, and (3) pinning of vortex strings with $F_L \| ab$. The relative relevance of these three contributions in real systems will strongly depend on the actual microstructure of the textured ceramics. In this work, by using the very same samples as in our previous work,[5] we present an accurate analysis of the flux-pinning mechanisms existing in these materials when the external magnetic field is applied parallel to the *ab* planes ($H \| ab$).

The anisotropy of the critical currents in YBCO single crystals and thin films has already been analyzed by several authors[7] and it has been clearly stated that when the Lorentz force is perpendicular to the *ab* planes the critical currents appear to be largely dominated by the intrinsic pinning mechanism pointed out by Tachiki and Takahashi[8] as a characteristic feature of layered high-temperature superconductors. In the present work, however, we will focus our analysis on the case when the Lorentz force lies parallel to the *ab* plane, i.e., the analysis of the influence of the microstructure on $J_c^c(H \| ab)$ is our main concern. Actually, the understanding of the behavior of this particular component of the critical current bears strong interest since it is directly related to the modifications of the microstructure ceramics through processing treatments and it is not masked by the strong contribution of the intrinsic pinning. We also note that transport critical current measurements of J_c^c are very scarce up to now while it may be easily investigated through magnetization measurements by using the anisotropic Beam model.

We will show that 123/211 interface pinning is still an effective pinning mechanism in this magnetic-field orientation resembling the correlated disorder behavior observed in the $H \| c$ orientation. Nevertheless, in this case, other defects not related to 123/211 interface and which we associate with the linear and planar defects lying parallel to the *ab* plane (stacking faults and dislocations) are also of relevance for all the investigated samples. Finally, we also evaluate the contribution of the twin planes to J_c^c when H lies parallel to them. Through a detailed quantification of the pinning contribution of these defects we have been able to infer the source of the critical current anisotropy in these materials.

II. EXPERIMENT

The preparation and microstructural characterization of the samples studied in the present investigation has been largely described in previous works.[2,4,9] Essentially, a Bridgman growth technique has been used to obtain single-domain samples having difference concentration and size of 211 particles. The range of compositions investigated extends from 4 to 38% of 211 in weight and the minimum mean size reached up to now is about 0.5 μm.[2,9] As we described in our previous work, the actual content of 211 phase in the samples was determined by measurements of high-temperature paramagnetic susceptibility which displays a Curie-Weiss law arising from the 211 particles. Only in this way can a meaningful scaling of the superconducting properties, with the amount of interface between the 123 matrix and the 211 precipitates, be reached.[5] A quantitative measure of the 123/211 interface may be represented through the parameter V/d, i.e., the ratio of the volume percentage of 211 phase and the mean diameter of the 211 precipitates determined by image analysis of SEM photographs.[2,9]

The inductive critical currents have been determined from isothermal and temperature dependent magnetization measurements carried out with a superconducting quantum interference device magnetometer provided with 5.5 T and by using an extraction magnetometer at the Service National des Champs Intenses (Grenoble) of up to 22 T. These measurements were performed on parallepipedic samples of about $2 \times 1.5 \times 0.5$ mm^3. The magnetic field was applied parallel to the *ab* plane ($H \| ab$) and out of the {110} twin planes, unless indicated otherwise, to avoid the contribution of twin boundaries to flux pinning.[10–12] The anisotropic Bean model has been used to compute J_c^c when the magnetic field is oriented parallel to one of its edges *b*, and the direction *c* is parallel to the *c* axis:[13]

$$\Delta M = \frac{J_c^c a}{20}\left(1 - \frac{a J_c^c}{3 c J_c^{ab}}\right), \tag{1}$$

where ΔM is the irreversible magnetization in Gauss and $a \times b \times c$ is the sample volume.

If we take into account that these samples fulfill the condition $J_c^c a \ll J_c^{ab} c$, Eq. (1) is reduced to $J_c^c \approx 20 \Delta M / a$, a being the larger side of the sample surface perpendicular to the applied field. Therefore, we can actually determine $J_c^c(H,T)$, i.e., the critical current corresponding to a pinning force pointing parallel to the *ab* planes when the vortices also remain parallel to the *ab* planes. It is clear then that no interference with the intrinsic pinning mechanism[8] is present in our measurements. We must also stress that we have indeed verified that magnetic relaxation effects are not relevant in most of the investigated regions of the magnetic phase diagram (except for those very near to the irreversibility line). Therefore, our analysis of the field and temperature dependence of J_c^c is essentially unaffected by flux-creep effects.

The evaluation of the critical current contribution of twin boundaries was performed in one particular sample (28% 211 and $V/d \approx 2550$ cm^{-1}) by applying the magnetic field along {110} planes, within the *ab* plane, in a sample with a parallepipedic shape and its edge parallel to the {100} planes. In this case Eq. (1) should be generalized to our particular geometry. After a detailed reconsideration of the new geometrical features we have obtained the following generalized equation for a parallepiped $a \times b \times c$ sample when the magnetic field is directed at 45° from *a* and *b* axis and the *c* direction is along the *c* axis:

$$\Delta M = \frac{J_c^c a}{10}\left[1 - \left(\frac{2 J_c^c a}{3\sqrt{2} c J_c^{ab}}\right)\right] - \frac{J_c^c a^2}{30 b}\left[1 - \frac{J_c^c a}{c J_c^{ab}}(\sqrt{2} - 2)\right]. \tag{2}$$

Once again the condition $J_c^c a \ll J_c^{ab} c$ is fulfilled in our samples and thus Eq. (2) is reduced to $\Delta M = J_c^c (a/10 - a^2/30b)$ from which we have calculated J_c^c when the magnetic field is directed along the $\langle 110 \rangle$ directions.

Finally, it is worth mentioning that special care was taken in the oxygenation process of all our samples. As we have previously demonstrated,[14,15] the duration of the oxygenation step at 450 °C is crucial to reach optimum critical currents because either a deficient layered oxygenation persists when the process is too short[14] or an ageing process appears when the oxygenation is too long.[15] The concomitant microstruc-

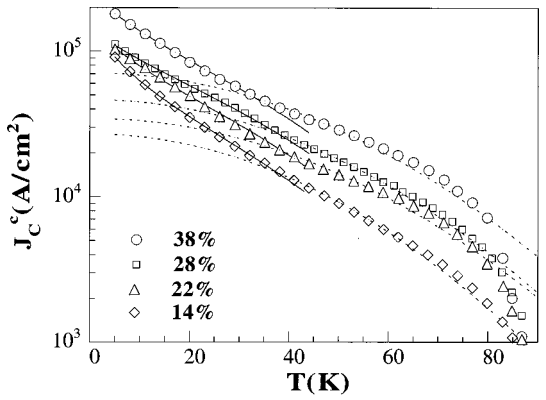

FIG. 1. Temperature dependence of J_c^c in textured ceramics samples with different concentration of 211 phase in self-field conditions. Continuous lines correspond to fits by using the collective-pinning–collective-creep theory [Eq. (4) in text]. Dashed lines correspond to fits using the correlated disorder pinning theory [Eq. (3) in text].

tural features may strongly affect the observed critical currents anisotropy. The optimum oxygenation treatment for each sample could be easily monitored by means of low-field susceptibility measurements with the field parallel to the *ab* planes. This was accomplished in all the samples investigated in the present work and so we safely assume that the measured critical currents are the optimized values for each composition in what concerns the oxygenation processes.

The critical currents of all the samples, having different concentration of 211 precipitates, were investigated by determining their temperature dependence at zero external magnetic field, $J_c^c(T)$, and their field dependence in isothermal conditions, $J_c^c(H)$. The experimental procedure for $J_c^c(T)$ determination was similar to that previously reported when $H\|c$ geometry,[5] i.e., the samples were field cooled under a magnetic field of 5.5 T down to 5 K where the magnetic field was decreased steadily to zero and then, the magnetization was measured while the temperature was slowly increased. Under these conditions the measurements of the persistent currents were actually performed under self-field conditions but because we choose carefully the geometry of the samples this field was never higher than $H_t = 2.5$–3 kOe and thus it had a small influence on the measured critical currents. Isothermal hysteresis loops were used to determine $J_c^c(H)$.

III. RESULTS

A. Dependence of the critical currents on the Y_2BaCuO_5 concentration

Figure 1 shows the temperature dependence of J_c^c measured in self-field conditions in several samples with different concentration of 211 phase. First of all, it should be noted that there is a clear correlation between the critical currents and the amount of 211 phase in the sample. Similarly to the $H\|c$ case,[5] this suggests that 123/211 interface pinning mechanism plays an important role at low fields. On the other hand, the temperature dependences of Fig. 1 reveal a softening above $T \approx 40$ K. This softening appears to be a phenomenon typical of melt-textured 123/211 composites. Measurements of critical currents for $H\|c$ in the same

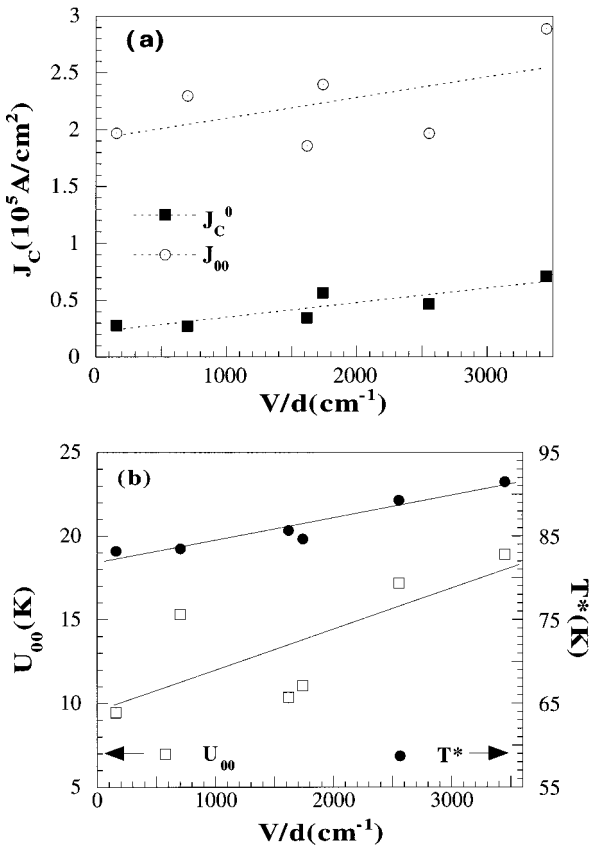

FIG. 2. Dependence on the 123/211 interface specific area of (a) the nonrelaxed critical currents J_c^0 and J_{00} included in Eqs. (3) and (5), respectively, and (b) the pinning energy terms T^* and U_{00} included in Eqs. (3) and (6), respectively. All the data correspond to measurements performed in self-field conditions.

samples here studied,[5] indicated that this softening could arise from a change in the dominating pinning centers. It was already suggested there that, 123/211 interfaces might have an enhanced contribution to flux pinning at high temperatures, because thermal activation enables the wandering of the vortex lines. Thus, depinning from the weaker pinning centers and bending is induced and vortices might be able to take as much advantage of 123/211 interface pinning as possible. Under those circumstances, the flux-line lattice is able to adjust itself to the random distribution of the 123/211 interfaces, resembling the behavior theoretically described by Nelson and Vinokur[16] as correlated disorder pinning and which typically occurs in ion-irradiated single-crystalline superconductors.[17,18] The occurrence of a similar phenomenon for the present field orientation ($H\|ab$) is very likely. The equation describing this pinning regime, when the concentration of vortices is below the so-called matching field, is given by the following expression:

$$J_c^c(T) = J_c^0 \exp -3(T/T^*)^2. \tag{3}$$

This fits by using this correlated disorderlike expression are indicated by dashed lines in Fig. 1. It is observed that this law reproduces nicely the experimental results in the temperature range 40 K$\leqslant T \leqslant$75 K, in close correspondence with the behavior observed in the $H\|c$ geometry.

Figures 2(a) and 2(b) show the dependence of the two

fitting parameters of Eq. (3), J_c^0 and T^* on the 123/211 interface specific area measured through the parameter V/d, where V is the volume percentage of 211 phase and d is the mean diameter of the 211 precipitates. The existence of a clear correlation between the parameters characterizing the strength of the 123/211 interface pinning, i.e., J_c^0 and T^*, and the interface specific area is evident. The linear relationship observed gives further support to the idea that 123/211 interfaces contribute to pinning in this field orientation where the Lorentz force is parallel to *ab* planes. We note, however, that the J_c^0 values do not extrapolate to zero when V/d goes to zero, as it was the case for the $H\|c$ geometry. This fact indicates that additional pinning contributions which are independent of the V/d parameter, should be considered. As will be discussed later, microstructural defects lying parallel to *ab* planes like in-plane dislocations, 1/6[301] partial dislocations surrounding stacking faults and in-plane lines surrounding the microcracks parallel to *ab* planes[2,4,19] might be good candidates.

At temperatures below ≈40 K, the critical currents do not follow the behavior predicted for correlated disorder [Eq. (3)]. Instead, experimental results are better described by the law expected for collective-pinning—collective-creep theory[20]

$$J_c^c(T)=\frac{J_{c0}}{[1+(\mu T/U_0)\ln(t/t_{\rm eff})]}. \tag{4}$$

In a similar way to the procedure used in $YBa_2Cu_3O_7$ single crystals[21] and melt-textured ceramics[5] in the $H\|c$ geometry, phenomenological laws for the temperature dependence of J_{c0} and U_0 can be used in Eq. (4). These laws are the following:

$$J_{c0}(T)=J_{00}\left[1-\left(\frac{T}{T_c}\right)^2\right]^n, \tag{5}$$

$$U_0(T)=U_{00}\left[1-\left(\frac{T}{T_c}\right)^2\right]^n. \tag{6}$$

These expressions are derived from the BCS temperature-dependent coherence length and the thermodynamic critical field. In order to minimize the number of fitting parameters, all the constants were fixed to those previously used in the $H\|c$ field orientation,[5] i.e., $\ln(t/t_{\rm eff})\cong 33$ and $n=3/2$. In this way the unique fitting parameters are the nonrelaxed critical current J_{00} and the pinning energy barrier at 0 K U_{00}.

The reason for the experimental agreement with these laws may arise from the fact that, when the temperature is lowered, thermal activation decreases and different pinning centers might become active in these melt-textured ceramics with such a rich microstructure. We should expect a coexistence of weak and strong pinning centers and thus the scenario may be more akin to that described by the collective-pinning theory. Instead, at high temperatures, only the strongest centers will remain active and a collective pinning theory will not be able to describe the experimental results.

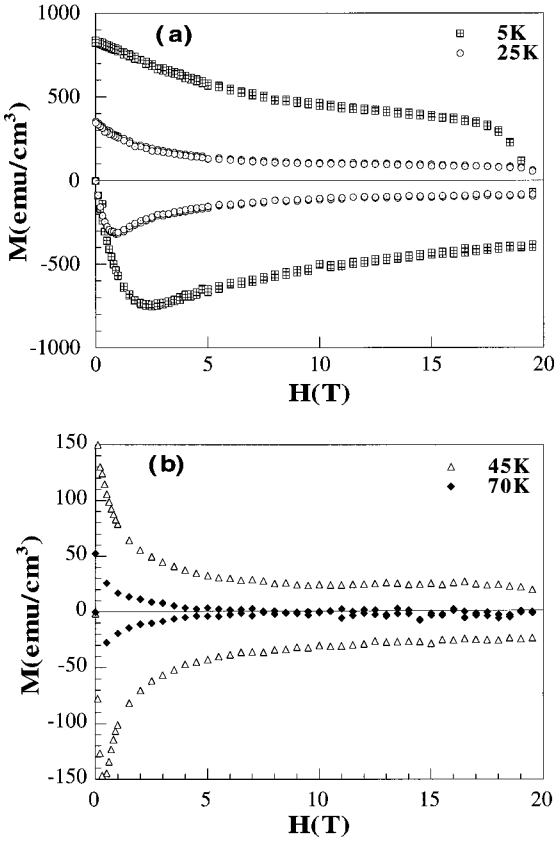

FIG. 3. Magnetization hysteresis loops measured at different temperatures with the magnetic-field-oriented $H\|ab$. All the measurements correspond to a sample with 30% of the 211 phase and $V/d\approx 3451\ \ {\rm cm}^{-1}$.

Figures 2(a) and 2(b) show that the J_{00} and U_{00} dependence on the V/d parameter. An overall increase of both J_{00} and U_{00} with the amount of 123/211 interface is observed, and similarly to the case of $H\|c$ orientation, the experimental points are more scattered than those corresponding to the correlated disorder pinning, i.e., J_c^0 and T^*. This suggests that the weak pinning centers, also contributing to pinning in this low-temperature region, are affected by a highest degree of randomness between the different samples that the strong pinning centers dominating at high temperatures. It is interesting to note that the maximum J_c^c values observed in our melt-textured samples approach those observed in untwined *a*-axis-oriented thin films.[7]

Figures 3(a) and 3(b) display typical isothermal hysteresis loops from which the field dependence of the critical currents has been evaluated. The corresponding critical currents are shown in a log-log plot in Figs. 4(a) and 4(b). From these plots it may be noted that in most of the investigated regions of the magnetic phase diagram, the field-dependent critical current density may be described by a power law $J_c^c \approx \beta^c H^{-\alpha}$. In addition and similarly to the temperature-dependent critical current measurements reported in Fig. 1, we observe an increase of J_c^c with the concentration of 211 particles. This gives further support to the idea that 123/211 interfaces do act as pinning centers in these melt-textured samples.

The temperature dependence of the power-law exponent of $J_c^c(H)$, α, is depicted in Fig. 5 for two representative

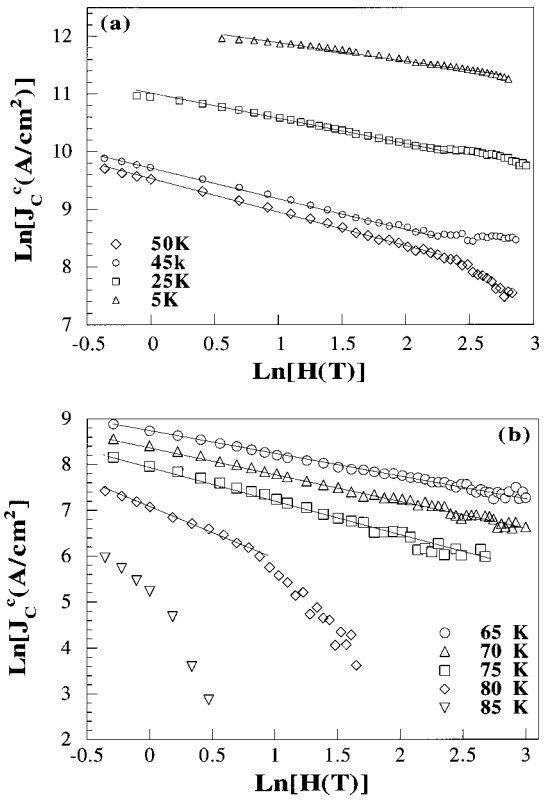

FIG. 4. (a) and (b) Field dependence of the inductive critical amounts J_c^c as calculated from the experimental hysteresis loops, assuming the validity of the anisotropic critical-state model. The continuous lines correspond to fits where a power-law dependence $J_c^c \propto H^{-\alpha}$ is found to be valid. All the data correspond to the sample with 30% 211 and $V/d \approx 3451\ \text{cm}^{-1}$.

samples. Note that while at low temperatures $\alpha \approx 0.3$, similarly to the value observed in the $H \| c$ orientation for melt-textured 123/211 composites[5] and 123 epitaxial thin films,[22] at higher temperatures and up to $T \approx 70$ K a plateau is observed around $\alpha \approx 0.5$. Above 70 K, this exponent suddenly increases towards $\alpha \approx 1.0$, the coefficient typically observed in the single vortex pinning regime by point defects.[23]

B. Twin boundary influence on the critical currents

The analysis of the influence of twin planes on the critical currents for $H \| ab$ was carried out in one particular sample,

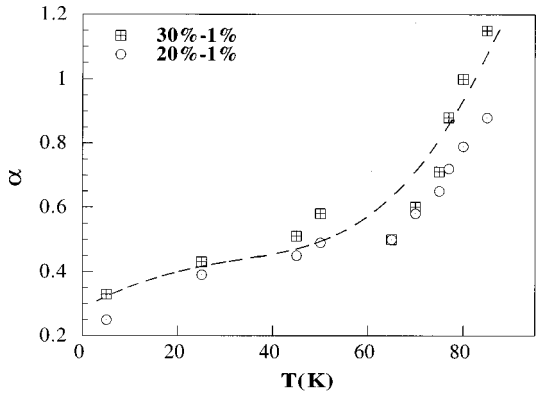

FIG. 5. Temperature dependence of the power-law coefficient α representing the field dependence of the critical currents $J_c^c \propto H^{-\alpha}$. The data correspond to samples with 211 additions of 30 and 20%.

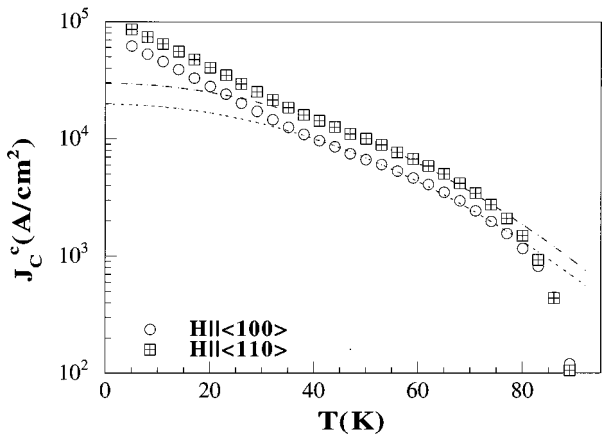

FIG. 6. Temperature dependence of the self-field critical currents $J_c^c(T)$ measured with the field orientations $H \| \langle 100 \rangle$ and $H \| \langle 110 \rangle$. Both measurements correspond to the same sample with 28% 211.

28% 211 with $V/d \approx 2550\ \text{cm}^{-1}$, through a comparison of the temperature and field dependence of the critical currents when $H \| \langle 110 \rangle$ and $H \| \langle 100 \rangle$. In Fig. 6 we compare the temperature dependence of $J_c^c(T)$ for those two particular field orientations. The calculation of J_c^c for $H \| \langle 110 \rangle$ has been performed following the extended critical-state analysis indicated before. Figure 6 also shows the fits corresponding to correlated disorder pinning [Eq. (3)] for both field orientations. As appreciated clearly, for H parallel to the twin planes J_c^c is higher than for $H \| \langle 100 \rangle$for all the temperature range except for temperatures approaching T_c.

Figure 7 shows the field dependence of $J_c^c(H)$ at different temperatures for the two orientations mentioned above and, once again, we can signal a clear enhancement of J_c^c when $H \| \langle 110 \rangle$. A $J_c^c \approx \beta^c H^{-\alpha}$ law may here also be applied. Furthermore, when the temperature dependence of the coefficient α is analyzed for $H \| \langle 110 \rangle$, a behavior similar to that represented in Fig. 5 is also found. We may then conclude that twin boundaries (TB's) are indeed effective defects for in-plane flux pinning when the Lorentz force remains parallel to the *ab* planes, in agreement with earlier analysis.[11]

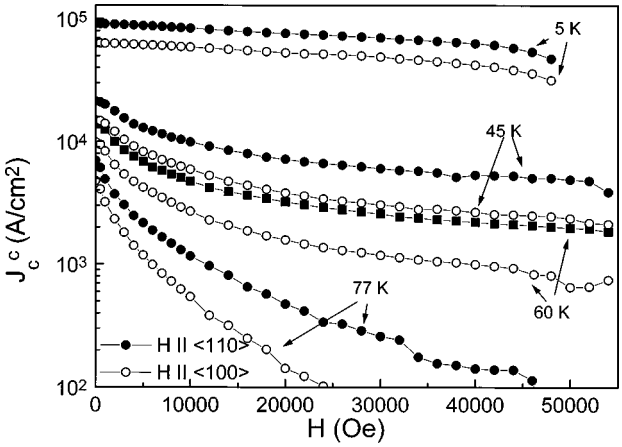

FIG. 7. Magneto-field dependence of the critical currents measured in a sample with 28% 211, at the temperatures indicated and with the magnetic field oriented along $\langle 100 \rangle$ and $\langle 110 \rangle$ directions.

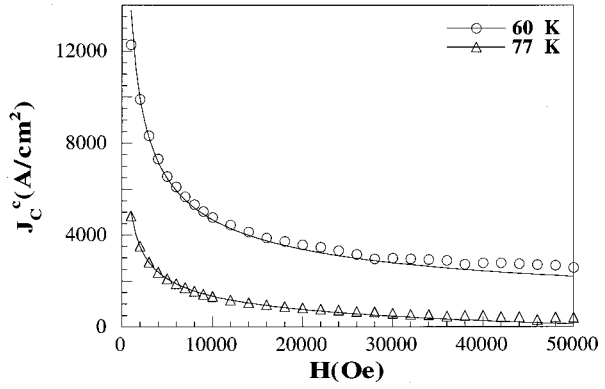

FIG. 8. Field dependence of the J_c^c critical currents measured at 60 and 77 K together with the fits by using a power-law dependence. It should be noted that a single law can reproduce all the examined magnetic-field range. The data correspond to a sample with 20% 211.

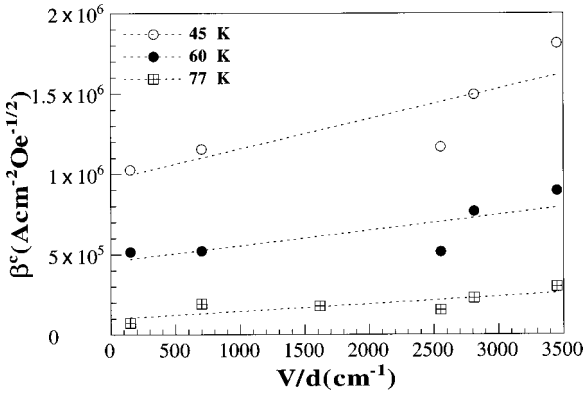

FIG. 9. Dependence on the 123/211 interface specific area V/d of the proportionality parameter β^c in the power-law field dependence of the critical currents represented by Eq. (7) in the text.

IV. DISCUSSION

A. Flux-pinning defects

In the previous paragraph we have conclusively shown that there is a correlation between the critical current of 123/211 melt-textured composites and the amount of 211 precipitates distributed in the 123 matrix and we have associated this correlation to interface pinning.

It was suggested by Murakami *et al.*[24] that the interface of 211 precipitates in melt-textured 123 superconductors may become active pinning centers through a core-pinning mechanism. Within this approximation, the field dependence of $J_c^{ab}(H)$ and $J_c^c(H)$ may be described by the laws

$$J_c^c = \frac{\pi \xi_c B_c^2 N_p d^2}{4\mu_0 \phi_0^{1/2} B^{1/2}} = \beta^c B^{-1/2}, \tag{7}$$

$$J_c^{ab} = \frac{\pi \xi_{ab} B_c^2 N_p d^2}{4\mu_0 \phi_0^{1/2} B^{1/2}} = \beta^{ab} B^{-1/2}, \tag{8}$$

where N_p is the number of 211 inclusions per unit volume and d is their mean size. Thus, J_c is proportional to $N_p d^2$, which corresponds to the quantity V/d, $V = N_p d^2$ being the volume fraction of the 211 precipitates. Note that the value observed for the coefficient α in the plateau regime of the field-dependent critical current of Fig. 5 was $\alpha \sim 0.5$, in agreement with Eq. (7). This agreement is further evidenced in Fig. 8 where the value of $\alpha = 0.5$ was directly imposed to the experimental data. Notice that for this magnetic-field orientation ($H \| ab$), the field dependence of $J_c^c(H)$ is indeed well represented by the same coefficient $\alpha = 0.5$ of Eq. (7) up to 5 T.

Furthermore, Eq. (7) predicts that the β^c coefficient varies linearly with the V/d parameter and this is, indeed, what is observed in Fig. 9. However, Fig. 9 identifies again a background contribution to β^c, in close similarity to what was also found in Fig. 2(a) for the J_c^{c0} term. Therefore, the results reported so far indicate that when $H \| ab$, both the temperature and field dependence of J_c^c, have simultaneously a contribution arising from 123/211 interfaces and a background contribution not related to the 123/211 precipitates.

Consequently we may write the following generalized expressions for J_c^c where both contributions are considered:

$$J_c^c(H) = (\beta^{cb} + \beta^{cI}) H^{-a} = [\beta^{cb} + \beta^{c0}(V/d)] H^{-a}, \tag{9}$$

$$J_c^c(T) = [(J_c^{0b} + J_c^{0I})] \exp -3(T/T^*)^2$$
$$= \{[J_c^{0b} + A^c(V/d)]\} \exp -3(T/T^*)^2, \tag{10}$$

where J_c^{0b} and β^{cb} correspond to the background values and A^c and β^{c0} are the slopes of the straight lines observed in Figs. 2(a) and 9, respectively, and hence all these parameters are independent of the interface parameter V/d. Note that both the background and the interface contribution are of the same order of magnitude, i.e., if we look at the zero-field contribution of J_c^c, as determined from the correlated disorder pinning fits [Eq. (10)]. The maximum contribution to J_c^c due to 123/211 interfaces is $J_c^{0I} \approx 5 \times 10^4$ A/cm^2, while the background value amounts $J_c^{0b} \approx 2 \times 10^4$ A/cm^2.

Now, having established that two different source of flux pinning exist in 123/211 composites when the vortices lie along the *ab* planes, the issue is to identify the defects responsible for the second identified mechanism, i.e., the background contribution. To answer this question the fact that the corresponding defects should have a field-dependent contribution to J_c^c similar to that of the 123/211 interfaces, since a unique $J_c^c \approx \beta H^{-\alpha}$ law holds over all the investigated field range, should be taken into account. This actually restricts the nature of defects to be considered. Furthermore, this background contribution was not observed in the $H \| c$ configuration. Thus, it is very likely that the corresponding defects will be linear and planar defects confined in the *ab* planes. The main candidates to become effective pinning centers when $H \| ab$ and $F_L \| ab$, are the in-plane dislocations and 1/6[301] partial dislocations surrounding the stacking faults, if we do not consider for the moment the twin boundaries.[2,4,19] All these defects have been systematically observed by TEM in 123/211 composites in large numbers so that they might account for the non-negligible background contribution observed.

In addition, the in-plane linear defects lying parallel to the *ab* planes have shown to have a tendency to be directed

along the {100} direction.[2] In the case of dislocations, the main reason seems to be the elastic interaction with preexisting defects such as twin boundaries.[25] For partial dislocations, it has been experimentally observed that the growth of stacking faults during the low-temperature oxygenation process is anisotropic and in the form of long fingerlike figures.[2,15,19] In both cases, fragments of vortices might become pinned in short segments at the core of the linear defects showing a behavior $J_c^c \propto B^{-1/2}$.[23,26] In-plane dislocations and stacking faults have been already considered as potential flux-pinning candidates in 123/211 ceramics even when $H \| c$.[27–29]

We may now extend our analysis of the temperature and field dependence of the critical current J_c^c to the case where twin boundaries are considered as well. A new term arising from twin boundary pinning should be included in Eqs. (9) and (10):

$$J_c^c(H) = [B^{cb} + \beta^{cI} + \beta^{c\mathrm{TB}}]H^{-\alpha}, \tag{11}$$

$$J_c^c(H) = [(J_c^{0b} + J_c^{0I} + J_c^{0\mathrm{TB}})[\exp(3(-T/T^*)^2], \tag{12}$$

where the $J_c^{0\mathrm{TB}} \neq 0$ only when H is oriented along {110} and T^* is assumed to be similar for the different microstructural defects. The effectiveness of TB's as a defect array leading to a Bose glass phase was already pointed out by Nelson and Vinokur[16] and experimentally verified, through anisotropic magnetoresistance,[10] anisotropic magnetization[11] and direct transport critical current measurements of J_c^c at 77 K.[12] A quantification of the different contributions to Eq. (12) gives the following values (see Figs. 2 and 6): $J_c^{0b} \approx 2\times10^4$ A/cm^2, $J_c^{0I} \approx 3\times10^4$ A/cm^2 and $J_c^{0\mathrm{TB}} \approx 1.5\times10^4$ A/cm^2 for the sample with $V/d \approx 2550$ cm^{-1} which indicates an increase of J_c^0 by twin boundaries of 30%. Therefore, we confirm that in the low-field single vortex pinning limit the three terms contribute to pin vortices but with an hierarchy between them.

A similar conclusion may be drawn comparing the β coefficients [Eq. (11)] describing the field dependence of the critical currents of the sample with 28% of 211 phase. In this case, an enhancement of $J_c \approx 40\%$ (see Fig. 7), independently of the temperature, has been found. However, it should be mentioned that on approaching the irreversibility line an enhanced divergence among the different critical currents appears, thus suggesting that the irreversibility line could strongly differ for {100} and {110} orientations, in agreement with the results reported by Sanfilippo *et al.*[12]

It is worth signaling that no traces of field saturation of $J_c^c(H)$ below the nominal matching field of the twin boundary array of planes, $B^* \approx 0.6$ T,[12] which corresponds to a mean separation between TB planes of about 1.000 Å, are observed. This is indeed the mean separation value observed in our TEM analysis of the present 123/211 ceramics.[4] In spite of that, $J_c^c(H)$ increases continuously below H^* at all investigated temperatures. Similar results have been found by other authors from inductive critical current measurements.[11] We should note at this stage that H^* remains well above the self-field H_t of our samples at 77 K and that $J_c^c(H)$ do not show any modification of the field dependence on crossing H^*. In conclusion, evidences of flux pinning of Josephson vortices at TB planes in 123/211 composites are given, but with a limited efficiency as compared to other existing defects.

B. Anisotropy of critical currents

We have shown that the critical currents for $H \| ab$, J_c^c, are about one order of magnitude smaller than the ones obtained for $H \| c$, J_c^{ab} (Ref. 5) for 123/211 melt-textured material, though this depends, among other factors, on the V/d value of the specific sample. In order to study the anisotropy of J_c, one might initially just determine the ratio between the two experimental J_c's, i.e., J_c^{ab}/J_c^c. However, this ratio will account for the intrinsic anisotropy of the material, the different nature of the vortices (i.e., Josephson or Abrikosov) and also for the different microstructural defect contributions on J_c^c and J_c^{ab} and their corresponding field dependences. This will result in a very complex analysis of the anisotropy. In the following, we will analyze separately the different contributions.

Initially we will try to infer on the nature of the anisotropy of the material, previously to the consideration of the anisotropic nature of the microstructural defects. In this case, we define an anisotropy ratio by dividing the two slopes A^{ab} and A^c of the linear relationship between J_c^0 and V/d [see Fig. 2(a) and Eq. (10)]. This anisotropy ratio, A^{ab}/A^c is independent of the linear and planar defects and it should only account for the intrinsic anisotropy of the material or the different nature of the vortices generated when $H \| c$ or $H \| ab$ (Abrikosov or Josephson, respectively) if spherical 211 particles are assumed. Figure 10(a) shows the $J_c^0(V/d)$ dependence for the two cases, $H \| ab$ and $H \| c$, from which the values $A^{ab} = 203$ A/cm and $A^c = 14.5$ A/cm have been determined. Therefore, the anisotropic ratio is $A^{ab}/A^c \approx 14$. This is twice the expected value ($\xi_{ab}/\xi_c \approx 7$), assuming that anisotropic Abrikosov vortices become pinned by a δT_c core pinning mechanism at the 123/211 interfaces, as described by Eqs. (7) and (8).[23,24] We note that this ratio could be even greater if we consider that the actual concentration of in-plane defects could slightly increase with V/d and thus the real contribution from the 211 interfaces when $H \| ab$ would be correspondingly smaller. It is worth it to emphasize, however, that the anisotropy ratios deduced from our analysis are very similar to those reported by Kuhn *et al.*[30] after magneto-optic flux penetration measurements in similar melt-texture 123/211 ceramics. Single-crystalline $YBa_2Cu_3O_7$ samples display much higher critical current anisotropy ratios [$J_c^{ab}(H \| c)/J_c^c(H \| ab) \approx 68$ (Ref. 31)], thus indicating that completely different pinning mechanisms hold in both cases.

This seems to indicate then that the coreless Josephson vortices are actually less effectively pinned than the Abrikosov vortices. A similar conclusion for point pinning centers was recently drawn by Berghuis *et al.*[7] in their study of the anisotropy of J_c in thin films grown over vicinal substrates, where a clear separation of the contribution to pinning from pancake and Josephson vortices was achieved. Furthermore, the expectation of a reduced efficiency for single-vortex pinning of a Josephson vortex, as compared to Abrikosov vortices, was already theoretically discussed by Blatter *et al.*[6]

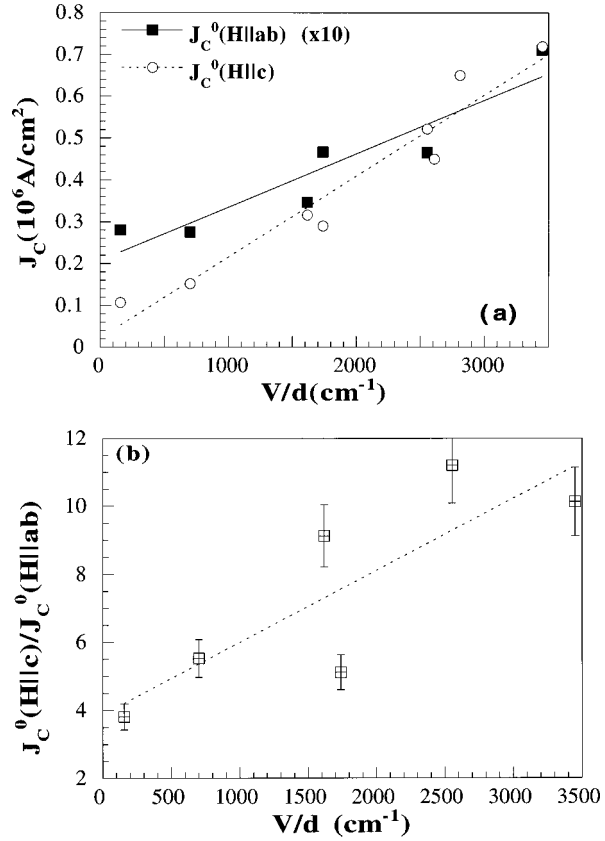

FIG. 10. (a) Dependence on the 123/211 interface specific area V/d of J_c^0 for $H\|c$ and J_c^0 for $H\|ab$ magnetic-field orientations. (b) Ratios $J_c^0(H\|c)/J_c^0(H\|ab)$ as a function of the 123/211 interface specific area.

Additionally, we should consider when deducing the pinning efficiency of the Josephson vortices from the anisotropy ratio described above, and specially for the case of melt-textured composites, the influence of the mosaic structure inherent to these ceramics. X-ray rocking curves of (001) reflections in 123/211 ceramics grown by Bridgman usually display a full width at half maximum $\Delta\theta \approx 2$–$3°$.[2,9] Therefore, it is necessary to estimate how this misorientation influences our previous assessment. The vortex structure of melt-textured materials, when the magnetic field is intended to be directed along the *ab* planes and when $T<T_{cr}$, the crossover temperature from a 2D to a 3D vortex nature, will always consist of a kinked configuration with some residual pancakes associated with the magnetic-field component parallel to the *c* axis and some segments of Josephson vortices (strings) directed along the *ab* planes.[6,7] We will show that even in this case, the pinning force contribution from the Abrikosov pancakes is very small in comparison with that of the Josephson strings, and therefore that the main contribution to the kinked vortex will come from the Josephson string segments. The pinning force associated with the segments of Josephson strings might be defined as $f_{st} \approx J_c^{st} \cdot L_{st}$, where J_c^{st} is determined at the magnetic field $H = H\cos(\Delta\theta/2)$, and where $(\Delta\theta/2)$ is the average misalignment of the magnetic field and the *ab* planes and L_{st} is the total string length. Similarly, the pinning force associated with the pancake vortex segments might be given by $f_{st} \approx J_c^{pk} \cdot L_{st}$, where now J_c^{pk} is determined at $H = H\sin(\Delta\theta/2)$ and L_{pk} is the total pancake length. Thus, since $L_{pk}/L_{st} \approx \tan(\Delta\theta/2)$, the ratio of the two pinning forces will be given by

$$\frac{f_p^{pk}}{f_p^{st}} = \frac{J_c^{pk}\sin(\Delta\theta)}{J_c^{st}}. \tag{13}$$

Using the J_c experimental values obtained in our samples for 3 T<H<5 T and 40 K<T<70 K and $\Delta\theta \approx 2$–$3°$, a value of $f_p^{pk}/f_p^{st} \approx 0.1$ is estimated. This confirms that the main contribution to the J_c^c values previously calculated through the Beam model, arises mainly from Josephson vortices. Then, it can be concluded that our results also seem to indicate that Josephson vortices exhibit a reduced pinning efficiency in comparison to what should be expected from an anisotropic Abrikosov vortex in agreement with Refs. 6 and 7.

As a last remark we should also comment on the origin of the sudden increase of the power-law coefficient α when increasing temperature (Fig. 5). As mentioned before, the vortex structure of $YBa_2Cu_3O_7$ displays a 2D-3D transition at $T_{cr} \approx 80$ K when the condition $\xi_c = d/\sqrt{2}$ is fulfilled. It is then tempting to interpret that when the low-temperature kinked vortices become again linear at $T>T_{cr}$ the effectiveness of the pinning mechanisms described above break down and a behavior more akin to that observed in materials with point defects becomes effective, thus leading at low fields in the single vortex pinning regime to a power-law field dependence with $\alpha \approx 1$.[23] Additionally, at these high temperatures a new behavior is evidenced characterized by a faster field dependence of J_c^c [Fig. 4(b)]. This probably indicates a crossover to a collective-pinning regime when approaching the irreversibility line.

Finally, we close by discussing the real meaning of determining the anisotropy of the critical currents, J_c^{ab}/J_c^c in melt-textured 123/211 superconductors. We have shown that mainly two contributions can be ascribed to J_c^c, the 123/211 isotropic interface pinning and the background associated with anisotropic linear and planar defects. Instead, only one contribution was assigned to J_c^{ab} at low fields:[5] the isotropic interface pinning. This indicates that in general the ratio J_c^{ab}/J_c^c is influenced by the morphological anisotropy of the linear and planar defects, by the intrinsic anisotropy of vortices in $YBa_2Cu_3O_7$ and by their corresponding field and temperature dependences. In particular in Fig. 10(b) we display the zero-field ratio $J_c^0(H\|c)/J_c^0(H\|ab)$ as a function of V/d which according to Eq. (3) is temperature independent. As it may be observed this ratio increases with V/d. At large values of interface area V/d the influence of linear in-plane defects is minimized, whereas the opposite occurs in the limit of small V/d values. In the former case, the ratio $J_c^0(H\|c)/J_c^0(H\|ab)$ will reflect mainly the intrinsic nature of vortices pinned at the interface and it should extrapolate to $J_c^0(H\|c)/J_c^0(H\|ab) \approx 14$, owing to the observed ratio of the slopes in Fig. 10(a).

V. CONCLUSIONS

The main objective of our experimental investigation was to analyze the sources of the anisotropic pinning in melt-textured 123/211 composites and to relate them to the ob-

served microstructure. Particularly, it was very appealing to elucidate if the intrinsic differential nature of the vortices when $H \| ab$, which must be described in terms of Josephson strings, leads also to a different behavior concerning flux pinning by defects.

A careful analysis of the temperature and field dependence of the critical currents, as a function of the amount of 123/211 interface, has evidenced in a consistent way that Josephson strings are pinned both by the precipitates and by additional in-plane linear defects. The relative contribution of the latter, however, is progressively reduced when the concentration of 211 precipitates is increased. At our maximum doping level the single vortex pinning contribution arising from the interface is 250% higher than that associated to the linear defects such as dislocations and partial dislocations surrounding the stacking faults.

The effectiveness of the interface pinning mechanism for Josephson strings has been also evaluated. It has been found that the pinning energy of a Josephson vortex is reduced by about 50% as compared to that expected for an anisotropic Abrikosov vortex when core pinning is considered. A similar reduction ratio for point defects in thin films has been recently reported[7] and was previously postulated theoretically by Blatter *et al.*[6]

Within this context the anisotropy of the low-field critical currents has been shown to depend strongly on the concentration of 211 particles and it is actually a reflection of the balance between two different terms: (1) Flux pinning by in-plane defects like dislocations and partial dislocations which are active for all the compositions of melt-textured 123/211 composites, and (2) a depressed effectiveness of Josephson strings to become pinned at the 123/211 interfaces. For these reasons, the significance of the experimental observation of modified anisotropy ratios must be taken with extreme caution.

Finally, we have also estimated, for a particular composition, the contribution of twin boundary planes to pin coreless Josephson vortices. This has been done through a comparison of the observed temperature and field dependence of the critical currents when the magnetic field is directed either along $\langle 110 \rangle$ or $\langle 100 \rangle$ directions. In a particular sample, having 28% of 211 phase, it was found that J_c^c may be increased by 30–40% and hence, it may be concluded that these planar defects behave as a source of effective correlated disorder for pinning in the $H \| ab$ direction. Overall, a hierarchy of the three main defects encountered in 123/211 composites as active pinning centers when $H \| ab$ has been established.

The quantitative evaluation of the pinning mechanisms in correlation with the microstructural defects identified by TEM helps to clarify the relevance of these defects and hence to develop more efficient material processing techniques to optimize the superconducting properties.

ACKNOWLEDGMENTS

The research reported in this work has been supported by CICYT (MAT95-0742), Programa MIDAS (Red Eléctrica de España, 93-2331), Generalitat de Catalunya, and EU-Large Scientific Facilities. T. P. wishes to thank Ministerio de Educación y Cultura for financial support.

[1] S. Jin, T. H. Tiefel, R. C. Sherwood, M. E. Davis, R. B. van Dover, G. W. Kammlott, R. A. Fastnacht, and H. D. Keith, Appl. Phys. Lett. **52**, 2074 (1988); K. Salama, V. Selvamanickkan, and D. F. Lee, in *Processing and Properties of High-T_c Superconductors*, edited by Sungho Jin (World Scientific, Singapore, 1993), Vol. 1, Chap. 5, pp. 155–211; M. Murakami, *ibid.*, Chap. 6, pp. 215–268; P. McGuinn, in *High Temperature Superconducting Materials Science and Engineering*, edited by Donglu Shi (Elsevier Science, Amsterdam, 1995), Chap. 8, pp. 345–382.

[2] F. Sandiumenge, B. Martínez, and X. Obradors, Supercond. Sci. Technol. **10**, A93 (1997).

[3] Y. Zhu, in *High Temperature Superconducting Materials Science and Engineering* (Ref. 1), Chap. 5, pp. 199–258.

[4] F. Sandiumenge, S. Piñol, X. Obradors, E. Snoeck, and Ch. Roucau, Phys. Rev. B **50**, 7032 (1994).

[5] B. Martínez, X. Obradors, A. Gou, V. Gomis, S. Piñol, J. Fontcuberta, and H. Van Tol, Phys. Rev. B **53**, 2797 (1996).

[6] G. Blater, M. V. Feigel'man, V. B. Geshkenbein, A. I. Larkin, and V. M. Vinokur, Rev. Mod. Phys. **66**, 1125 (1994).

[7] P. Berghuis, E. Di Bartolomeo, G. A. Wagner, and J. E. Evetts, Phys. Rev. Lett. **79**, 2332 (1997); Z. Trajanovic, C. J. Lobb, M. Rajeswari, I. Takeuchi, C. Kwon, and T. Venkatesan, Phys. Rev. B **56**, 925 (1997).

[8] M. Tachiki and S. Takahashi, Solid State Commun. **70**, 291 (1989); **72**, 1633 (1989).

[9] R. Yu, V. Gomis, F. Sandiumenge, B. Martínez, N. Vilalta, S. Piñol, and X. Obradors, Physica C **290**, 161 (1997); S. Piñol, F. Sandiumenge, B. Martínez, V. Gomis, J. Fontcuberta, X. Obradors, E. Snoeck, and Ch. Roucau, Appl. Phys. Lett. **65**, 1448 (1994).

[10] W. K. Kwok, U. Welp, G. W. Crabtree, K. G. Vandervoort, R. Hulscher, and J. Z. Liu, Phys. Rev. Lett. **64**, 966 (1990).

[11] H. Fujimoto, T. Taguchi, M. Murakami, N. Nakamura, and N. Koshizuka, Cryogenics **32**, 954 (1992); M. Oussena, P. A. J. de Groot, and S. J. Porter, Phys. Rev. B **51**, 1389 (1995); M. Oussena *et al.*, Phys. Rev. Lett. **76**, 2559 (1996); A. A. Zhukov, G. K. Perkins, J. V. Thomas, A. D. Caplin, H. Kupfer, and T. Wolf, Phys. Rev. B **56**, 3481 (1997).

[12] S. Sanfilippo, D. Bourgault, C. Villard, R. Tournier, P. Gautier Picard, E. Beaugnon, A. Sulpice, Th. Fournier, and P. Germi, Europhys. Lett. **39**, 657 (1997).

[13] E. M. Gyorgy, R. B. van Dover, K. A. Jackson, L. F. Schneemeyer, and J. V. Waszczak, Appl. Phys. Lett. **55**, 283 (1989); H. P. Wiesinger, F. M. Sauerzopf, and H. W. Weber, Physica C **203**, 121 (1992).

[14] B. Martínez, V. Gomis, S. Piñol, I. Catalan, J. Fontcuberta, and X. Obradors, Appl. Phys. Lett. **63**, 3081 (1992).

[15] B. Martínez, F. Sandiumenge, S. Piñol, N. Vilalta, J. Fontcuberta, and X. Obradors, Appl. Phys. Lett. **66**, 772 (1995); F. Sandiumenge, N. Vilalta, S. Piñol, B. Martínez, and X. Obradors, Phys. Rev. B **51**, 6645 (1995).

[16] D. R. Nelson and V. M. Vinokur, Phys. Rev. Lett. **68**, 2398 (1992); Phys. Rev. B **48**, 13 060 (1993).

[17] V. V. Moshchalkov, V. V. Metlushko, G. Güntherodt, I. N. Goncharov, A. Yu. Didyk, and Y. Bruynseraede, Phys. Rev. B **50**, 639 (1994).
[18] L. Krusin-Elbaum, L. Civale, J. R. Thomson, and C. Feild, Phys. Rev. B **53**, 11 744 (1996).
[19] F. Sandiumenge, N. Vilalta, Y. Maniette, and X. Obradors, Appl. Phys. Lett. **70**, 2192 (1997).
[20] M. V. Feigel'man, V. B. Geshkenbein, and V. M. Vinokur, Phys. Rev. B **43**, 6263 (1991); M. V. Feigel'man, and V. M. Vinokur, *ibid.* **41**, 8986 (1990).
[21] J. R. Thompson, Yang Ren Sun, L. Civale, A. P. Malozenmoff, M. W. McElfresh, A. D. Marwick, and F. Holtzberg, Phys. Rev. B **47**, 14 440 (1993).
[22] R. Griessen, Wen Hai-hu, A. J. J. Van Dalen, B. Dam, J. Rector, H. G. Schnack, S. Libbrecht, E. Osquiguil, and Y. Bruynseraede, Phys. Rev. Lett. **72**, 1910 (1994); Wen Hai-hu, H. G. Schnack, R. Griessen, B. Dam, and J. Rector, Physica C **241**, 353 (1995).
[23] A. M. Campbell and J. E. Evetts, Adv. Phys. **21**, 199 (1972).
[24] M Murakami, S. Gotoh, H. Fujimoto, K. Yamaguchi, N. Koshizuka, and S. Tanaka, Supercond. Sci. Technol. **4**, S43 (1991).
[25] J Rabier and M. F. Denanot, Philos. Mag. A **65**, 427 (1992).
[26] D. Dew-Hughes and M. J. Witcomb, Philos. Mag. **26**, 73 (1972).
[27] V. Selvamanickam, M. Mironova, S. Son, and K. Salama, Physica C **208**, 238 (1993).
[28] M. Ullrich, D. Müller, W. Mexner, M. Steins, K. Heinemann, and H. C. Freyhardt, Phys. Rev. B **48**, 7513 (1993).
[29] P. X. Zhang, L. Zhou, P. Ji, W. M. Bian, X. Z. Wu, and Z. H. Lai, Supercond. Sci. Technol. **8**, 15 (1995); P. X. Zhang, H. W. Weber, and L. Zhou, *ibid.* **8**, 701 (1995).
[30] H. Kuhn, M. Glueker, B. Ludescher, and H. Kronmuller, J. Appl. Phys. **74**, 3307 (1993).
[31] K. Schönmann, B. Secbacker, and K. Andres, Physica C **184**, 41 (1991).